Mathematical Models of Proprioceptors. II. Structure and Function of the Golgi Tendon Organ

Milana P. Mileusnic and Gerald E. Loeb

J Neurophysiol 96:1789-1802, 2006. First published May 3, 2006; doi:10.1152/jn.00869.2005

J Neurophysiol 96: 1789–1802, 2006.
First published May 3, 2006; doi:10.1152/jn.00869.2005.

Mathematical Models of Proprioceptors. II. Structure and Function of the Golgi Tendon Organ

Milana P. Mileusnic and Gerald E. Loeb

Department of Biomedical Engineering, Alfred E. Mann Institute for Biomedical Engineering, University of Southern California, Los Angeles, California

Submitted 18 August 2005; accepted in final form 2 March 2006

Mileusnic, Milana P. and Gerald E. Loeb. Mathematical models of proprioceptors. II. Structure and function of the Golgi tendon organ. *J Neurophysiol* 96: 1789–1802, 2006. First published May 3, 2006; doi:10.1152/jn.00869.2005. We developed a physiologically realistic mathematical model of the Golgi tendon organ (GTO) whose elements correspond to anatomical features of the biological receptor. The mechanical interactions of these elements enable it to capture all salient aspects of GTO afferent behavior reported in the literature. The model accurately describes the GTO's static and dynamic responses to activation of single motor units whose muscle fibers insert into the GTO, including the different static and dynamic sensitivities that exist for different types of muscle fibers (S, FR, and FF). Furthermore, it captures the phenomena of self- and cross-adaptation wherein the GTO dynamic response during motor unit activation is reduced by prior activation of the same or a different motor unit, respectively. The model demonstrates various degrees of nonlinear summation of GTO responses resulting from simultaneous activation of multiple motor units. Similarly to the biological GTO, the model suggests that the activation of every additional motor unit to already active motor units that influence the receptor will have a progressively weaker incremental effect on the GTO afferent activity. Finally, the proportional relationship between the cross-adaptation and summation recorded for various pairs of motor units was captured by the model, but only by incorporating a particular type of occlusion between multiple transduction regions that were previously suggested. This occlusion mechanism is consistent with the anatomy of the afferent innervation and its arrangement with respect to the collagen strands inserting into the GTO.

INTRODUCTION

Golgi tendon organs (GTO) are tension-sensitive mechanoreceptors found in mammalian skeletal muscles that supply the CNS with information regarding active muscle tension by their Ib afferents. The number of GTOs varies widely among muscles but in most cases is somewhat smaller than the number of muscle spindles in the same muscle, generally in the range of 10–100 (Jami 1992). The GTOs are most commonly located at the junctions between the muscle fibers and the collagen strands composing tendons and aponeuroses (Fig. 1) (Golgi 1878, 1880); in rare cases they have been reported within tendons themselves (in the material of Pang, quoted by Barker 1974). The distribution of the GTOs is uneven and there is a tendency for them to lie deep in the central zone of the muscle, also known as the muscle core (Lund et al. 1978; Richmond and Stuart 1985; Swett and Eldred 1960). In muscles with nonhomogeneous distribution of extrafusal fiber types [e.g. medial gastrocnemius (MG)], this is the area associated with the largest percentage of slow oxidative fibers responsible for low-force, nonfatiguing tasks (Burke and Tsairis 1973).

The GTO receptor consists of bundles of collagen fibers that connect small fascicles of muscle to the whole muscle tendon or aponeurosis. In other words, the GTO is placed in series between muscle fibers ("muscle end") and tendon and aponeurosis ("tendon end"), contrary to the muscle spindle that lies in parallel with extrafusal muscle fibers. The number of muscle fibers that insert into a single GTO varies, but in most cases is between three and 50 fibers (only 5% of receptors are attached to more than 25 fibers; Jami 1992).

Each GTO receptor is usually innervated by a single large, myelinated Ib afferent that enters the GTO capsule near its equator (Fig. 1). The Ib afferent typically travels to the center of the GTO capsule where it splits into two or sometimes more large myelinated branches (Nitatori 1988; Schoultz and Swett 1973). One afferent branch courses toward the GTO's proximal (muscle) end, the other toward the distal (tendon) end. The two main branches repeatedly divide further into smaller branches until giving rise to unmyelinated collateral branches that are intertwined among the collagen strands. The number of impulse-generating sites that exist in the GTO is unknown. Although there is no direct experimental evidence supporting the existence of multiple impulse-generating sites, the presence of at least two large myelinated branches within the receptor capsule makes it quite possible that GTO afferent activity results from interactions between more than one impulse-generating site (for more details see DISCUSSION).

The collagen within the GTO capsule is unevenly packed. The marginal areas of the GTO are typically occupied by densely packed collagen whose fibers run in parallel with one another and very rarely make contact with the GTO afferent endings (Fig. 1). The second type of collagen that typically occupies the GTO capsule lumen is innervated collagen (Nitatori 1988; Schoultz and Swett 1973). Toward the two ends (muscle and tendon end) this type of collagen is densely packed but as it approaches more central areas within the capsule it becomes loosely arranged, with its fibers no longer running in parallel but rather giving rise to a complex network where collagen fibrils belonging to different muscle fibers continuously divide, mix, and fuse with one another. The loosely packed collagen is densely innervated by GTO afferent endings whose axonal branches wind back and forth between

Address for reprint requests and other correspondence: M. P. Mileusnic, Alfred E. Mann Institute for Biomedical Engineering, Department of Biomedical Engineering, University of Southern California, 1042 Downey Way, Room DRB-B11, Los Angeles, CA 90089-1112 (E-mail: mileusni@usc.edu).

The costs of publication of this article were defrayed in part by the payment of page charges. The article must therefore be hereby marked "*advertisement*" in accordance with 18 U.S.C. Section 1734 solely to indicate this fact.

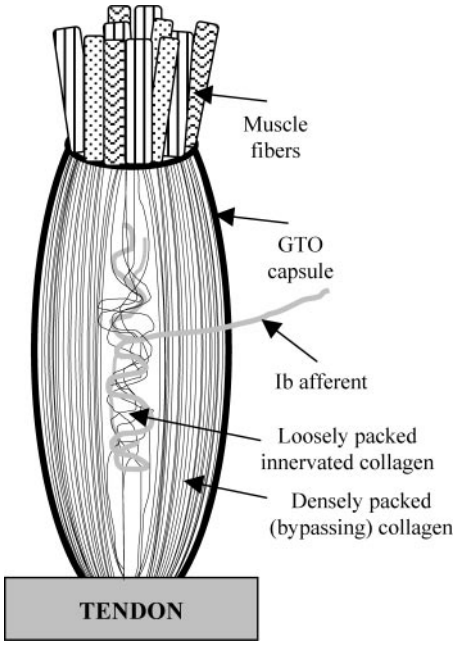

FIG. 1. Structure of the Golgi tendon organ (GTO). GTO receptor is located in series between the tendon and muscle fibers that insert into it. It is composed of 2 types of collagen: innervated collagen that occupies the capsule lumen and surrounds many afferent endings; and bypassing collagen that occupies the marginal areas of the GTO and lacks contact with GTO afferent endings. A single GTO afferent axon enters the GTO capsule about halfway between the GTO's proximal (muscle) and distal (tendon) end and travels into the middle of the capsule lumen, at which point it splits into 2 myelinated branches. One afferent branch courses toward the GTO's proximal end, the other toward the distal end. Two main branches repeatedly divide further into smaller branches until giving rise to unmyelinated collateral branches that are intertwined among the strands of innervated collagen.

and around collagen braids and repeatedly form dilations that expose large areas of their cell surface to neighboring collagen bundles (Schoultz and Swett 1972).

The activation of a motor unit (MU) with at least one muscle fiber inserting into the GTO straightens some of the loosely packed collagen strands, compressing and depolarizing the pressure-sensitive afferent endings and eventually resulting in initiation of action potentials in the Ib axon (Fukami and Wilkinson 1977). The experimental literature describes several peculiarities in GTO afferent behavior. After a sudden step activation of the MU, the GTO response consists of a burst (dynamic response) that gradually decays to a constant afferent firing (static response) (see Fig. 3). Although the GTO response depends on the tension that the MU's muscle fiber exerts on collagen strands attached to it, it also depends on the type of MU being activated. For example, MUs with small forces (slow MUs) as well as large forces (fast fatigable MUs) can produce similarly high discharge frequencies in tendon organs when activated (Gregory and Proske 1979). Several researchers also describe a phenomenon whereby a GTO's dynamic response during MU activation is decreased after prior activation of the same MU (self-adaptation) or a different MU (cross-adaptation) (Gregory and Proske 1979; Gregory et al. 1985). Furthermore, it was observed that the cumulative GTO response when multiple MUs are stimulated simultaneously in the GTO is lower than the sum of GTO responses that individual MUs produce when stimulated independently (Crago et al. 1982; Gregory and Proske 1979; Proske and Gregory 1980). Finally, during the activation of two MUs with fibers inserting into the GTO, researchers observed a proportional relationship between the amount of cross-adaptation and nonlinear summation (Gregory et al. 1985). In other words, a MU that has a stronger ability to cross-adapt another MU will contribute more of its firing to the cumulative GTO afferent response than a MU having the weaker ability to cross-adapt.

The aim of this study was to develop a model of the individual GTO that captures all physiologically salient aspects of its behavior. Properties such as the nonlinear relationship between force of a muscle fiber and its effects on afferent firing and nonlinear summation between simultaneously activated muscle fibers have led researchers to suggest that GTOs cannot provide accurate information about muscle force (Jami 1992). We have used this model to predict the relationships among recruitment, force, and aggregate GTO activity in muscles with realistic ensembles of MU and GTO distribution under various normal, pathological, and therapeutic conditions (Mileusnic and Loeb, unpublished observations).

METHODS

The Golgi tendon organ model

INPUT TO THE MODEL. Similarly to the biological GTO, the GTO model receives the tension input from multiple muscle fibers inserting into its capsule. Much of the literature on GTO physiology comes from the MG muscle of the cat, where each GTO has an average of 14.4 muscle fibers attaching at its muscle end plus 5.6 attaching to the side of the GTO capsule (Gregory 1990). For purposes of our model, we decided to include the fibers inserting into the capsule into the model and to treat them in the same manner as the fibers inserting at the muscle end (for reasoning see DISCUSSION). A MU having influence on the MG's GTO response has typically one or two fibers inserting into its capsule (an average of 1.6 muscle fibers; Gregory 1990). Therefore our model's input consists of tensions of 20 fibers that originate from 13 different MUs where an individual MU has one or two fibers inserting into the receptor's capsule.

STRUCTURE OF THE MODEL. A single muscle fiber inserting into the GTO was modeled as interacting with two types of collagen that can be found in the receptor's capsule (see Fig. 2*A*): bypassing collagen and innervated collagen. The *bypassing collagen* represents densely packed collagen that is attached to the muscle fiber inserting into the receptor but is not intertwined with afferent endings. The *innervated collagen* is densely packed at the capsular ends but becomes loosely arranged and intermingled with unmyelinated afferent endings in the middle of the capsule. Because the experimental literature suggests that such loosely packed collagen fibers (presumably originating from different muscle fibers) extensively intermingle with each other, the model included springlike elements from each muscle fiber that conveyed tension to common transduction zones. The phenomenon of cross-adaptation is the most direct consequence of such collagen packing.

Because at least two large myelinated branches are typically found within the GTO capsule, each innervating separate portions of the GTO's innervated collagen network (Nitatori 1988; Schoultz and Swett 1973), the model assumes the existence of two separate transduction zones (or two common innervated collagen networks), each having its own impulse-generating site. Inclusion of more than a single impulse-generating site in our model contributed to the nonlinear summation of GTO afferent responses that individual MUs produce when stimulated simultaneously. This feature proved to be essential to capture the proportional relationship between the cross-adaptation and summation during the two MU interactions (for more details see RESULTS and DISCUSSION).

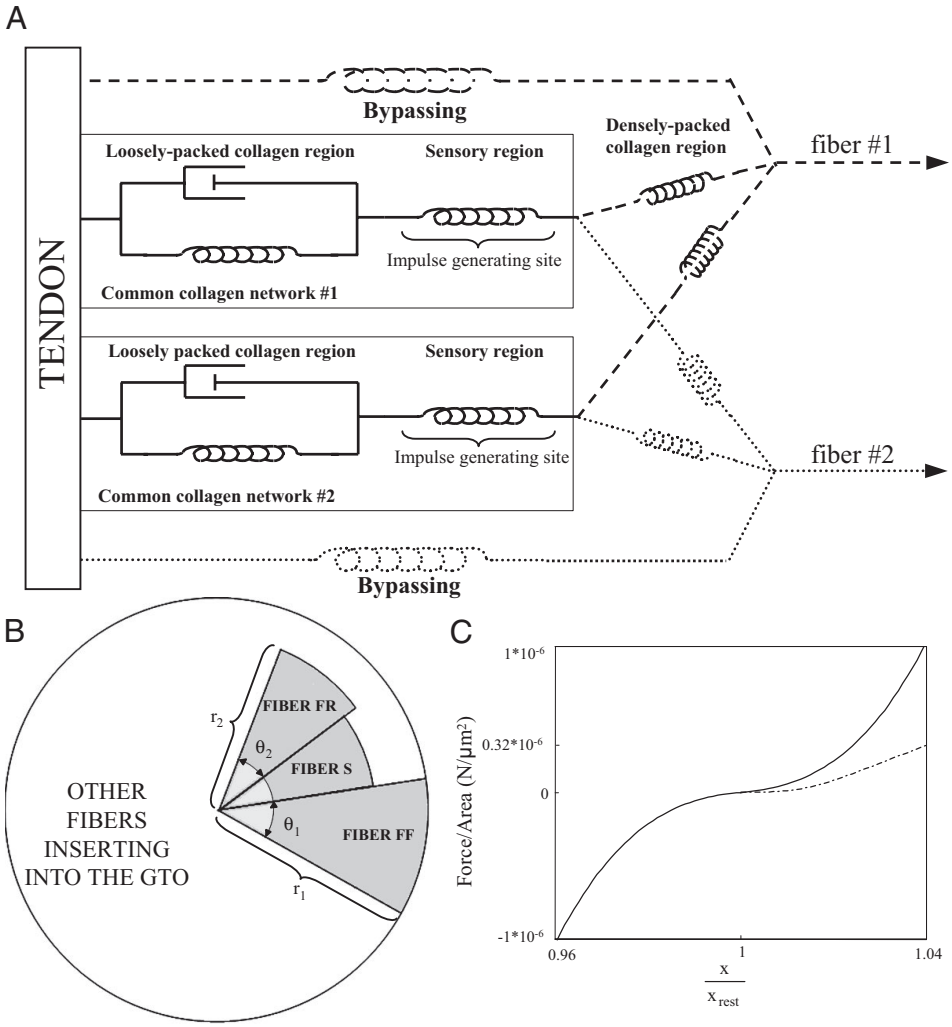

FIG. 2. GTO model. *A*: structure of the GTO model. For simplicity the figure represents only 2 of the many muscle fibers that insert into the GTO capsule. Each fiber has its collagen divided among bypassing and innervated collagen, which is then divided between 2 common collagen networks having separate impulse-generating sites. *B*: flower-shaped cross-sectional area of collagen within the GTO. Muscle fibers' collagen was assumed to be arranged in the manner of the flower petals where the fiber's collagen that occupies the central area of flower-shaped structure belongs to the innervated collagen type (light gray), whereas the more distally located collagen is of bypassing type (dark gray). For more details see the APPENDIX. *C*: collagen stress–strain relationship. Percentage collagen length change (x/x_{rest}) is plotted against the force per collagen cross-sectional area ($N/\mu m^2$). Broken line represents the stress–strain relationship for tendon and aponeurosis modeled by Brown et al. (1996), whereas the solid line is our estimate of collagen's stress–strain relationship (*Eq. 2*). Note that during the tetanic contraction (0.32×10^{-6} $N/\mu m^2$), the collagen is stretched by some 2.5% rather than 4%. Finally, note that we have assumed that the force to shorten the collagen by a specific amount is the same but of opposite sign as to lengthen it by the same amount.

Mathematically, the tension of a single fiber (T^f) that inserts into the GTO is split between the bypassing collagen (T^{f_bypass}) and two common collagen networks that are innervated (T^{f_com1} and T^{f_com2})

$$T^f = T^{f\_bypass} + T^{f\_com1} + T^{f\_com2} \quad (1)$$

Before deriving the tension equations for different sections of the GTO model, we will introduce the stress–strain properties of collagen that were used in modeling collagen throughout the GTO model. The incorporation of physiologically realistic, nonlinear properties for collagen also turned out to be essential to the performance of the model.

Stress–strain properties of collagen. The following collagen tension equation was designed to account for the stress–strain relationship for tendon and aponeurosis as reported in the experimental data (Brown et al. 1996; Scott and Loeb 1995) (Fig. 2*C*)

$$T^{col} = K^{col} \times A^{col} \times \text{sign}\,(x - x_{rest}) \times \left\{ \left[\frac{\text{abs}\,(x - x_{rest}) + x_{rest}}{x_{rest}} - 0.99 \right]^3 - 10^{-6} \right\} \quad (2)$$

where x and x_{rest} are collagen length and rest length, respectively. T^{col} represents the tension necessary to stretch a collagen strand having a cross-sectional area A^{col} by length equal to x/x_{rest}. K^{col} is a collagen coefficient in units of $N/\mu m^2$. Note that during the tetanic tension the model's collagen is stretched to some 2.5% rather than 4% of its rest length as suggested by Brown et al. (1996). The reasoning behind this is provided in *Parameter determination*. Also note that the force necessary to shorten the collagen was assumed to be of the same magnitude but opposite direction from the one to lengthen it.

Bypassing collagen. The muscle fiber's bypassing collagen was modeled as a spring having stress–strain properties typical of collagen (*Eq. 2*). The tension within the fiber's bypassing elements (T^{f_bypass}) was expressed as

$$T^{f\_bypass} = K^{col} \times A^{f\_bypass} \times \text{sign}\,(L^{f\_bypass} - L^{bypass}_{rest}) \times \left\{ \left[\frac{\text{abs}\,(L^{f\_bypass} - L^{bypass}_{rest}) + L^{bypass}_{rest}}{L^{bypass}_{rest}} - 0.99 \right]^3 - 10^{-6} \right\} \quad (3)$$

L^{f_bypass} and L^{bypass}_{rest} are the fiber's bypassing collagen length and bypassing collagen rest length, respectively. K^{col} is a collagen coefficient (in units of $N/\mu m^2$), whereas A^{f_bypass} is the cross-sectional area of fiber's collagen of the bypassing type (in units of μm^2) (for more details on how A^{f_bypass} is determined for different muscle fibers see the APPENDIX).

Innervated collagen. The collagen fibers attached to a given muscle fiber contribute qualitatively similar mechanical effects to each of the two common collagen networks, although the magnitude of their influence may differ. Thus the tension equations for two common collagen network systems are similar except that the fiber's contributions of its innervated collagen to each of the two networks might differ. Instead of writing the equations twice for the two systems we will designate the common collagen network terms that may potentially differ for two networks by X (where X can be 1 or 2).

The portion of the fiber's innervated collagen that is densely packed (lying close to two GTO ends) and inserts into X common collagen network was modeled as a collagen spring (cross-linking spring) (*Eq. 2*). This spring was then placed in series with the common collagen network, which consists of a sensory region and the loosely packed collagen region. The sensory region represents the collagen that is in direct contact with the sensory endings and whose stretch results in proportional distortion and transduction in the sensory endings. This was modeled as a collagen spring (*Eq. 2*). The loosely packed collagen within the X common collagen network consists of a collagen spring (*Eq. 2*) in parallel with a damper where the damper represents the ability of collagen strands within the network to gradually rearrange after the stretch. The viscosity may arise from sliding motion of the collagen fibers in the capsule, flow of axoplasm in the afferent endings squeezed by the collagen fibers, or a combination of the two. The viscosity was modeled as being dependent on the force being exerted on the loosely packed collagen; i.e., we assumed that a more highly stressed GTO would have a more highly ordered internal structure that would result in a higher viscosity. This was crucial in capturing the dynamic peak decay time to a progressively larger number of MUs (see *Nonlinear summation* in RESULTS; Fig. 5*A*).

The tension within the densely packed portion of the fiber's innervated collagen region (cross-linking spring) that inserts into GTO's X common collagen network T^{f_comX}) is

$$T^{f\_comX} = K^{col} \times P^{f\_comX} \times A^{f\_inner} \times \text{sign}\left[(L^{f\_bypass} - L^{comX}_{sens} - L^{comX}_{loose}) - (L^{bypass}_{rest} - L^{com}_{sens\_rest} - L^{com}_{loose\_rest})\right] \times \left(\left\{ \frac{\text{abs}\left[(L^{f\_bypass} - L^{comX}_{sens} - L^{comX}_{loose}) - (L^{bypass}_{rest} - L^{com}_{sens\_rest} - L^{com}_{loose\_rest})\right]}{L^{bypass}_{rest} - L^{com}_{sens\_rest} - L^{com}_{loose\_rest}} + \frac{L^{bypass}_{rest} - L^{com}_{sens\_rest} - L^{com}_{loose\_rest}}{L^{bypass}_{rest} - L^{com}_{sens\_rest} - L^{com}_{loose\_rest}} - 0.99 \right\}^3 - 10^{-6} \right) \quad (4)$$

L^{comX}_{sens} and L^{comX}_{loose} are X common collagen network's sensory and loosely packed regions' lengths, respectively, whereas their rest lengths are $L^{com}_{sens\_rest}$ and $L^{com}_{loose\_rest}$. A^{f_inner} is the cross-sectional area of the fiber's collagen that is of innervated collagen type (for more details on how to obtain A^{f_inner} see the APPENDIX), whereas P^{f_comX} is the percentage of muscle fiber's innervated collagen that contributes to the X common collagen network.

The tensions within the X common collagen network's sensory region and loosely packed collagen region are the same and are equal to the summation of the tensions within the densely packed innervated collagen region of all fibers that insert into X common collagen network ($\sum_{f=1}^{20} T^{f\_comX}$, where 20 represents for the number of muscle fibers that insert into the individual cat's MG GTO receptor). In other words, the tension within the X common collagen network's sensory region is

$$\sum_{f=1}^{20} T^{f\_comX} = K^{col} \times \sum_{f=1}^{20} (P^{f\_comX} \times A^{f\_inner}) \times \text{sign}\,(L^{comX}_{sens} - L^{com}_{sens\_rest}) \times \left\{ \left[\frac{\text{abs}\,(L^{comX}_{sens} - L^{com}_{sens\_rest}) + L^{com}_{sens\_rest}}{L^{com}_{sens\_rest}} - 0.99 \right]^3 - 10^{-6} \right\} \quad (5)$$

The tension within the X common collagen network's loosely packed collagen region is

$$\sum_{f=1}^{20} T^{f\_comX} = \text{abs}\,(B^{col} \times \sum_{f=1}^{20} T^{f\_comX})^a \times \sum_{f=1}^{20} (P^{f\_comX} \times A^{f\_inner}) \times \left(\frac{L^{comX}_{loose}}{L^{com}_{loose\_rest}} \right) + K^{col} \times \sum_{f=1}^{20} (P^{f\_comX} \times A^{f\_inner}) \times \text{sign}\,(L^{comX}_{loose} - L^{com}_{loose\_rest}) \times \left\{ \left[\frac{\text{abs}\,(L^{comX}_{loose} - L^{com}_{loose\_rest}) + L^{com}_{loose\_rest}}{L^{com}_{loose\_rest}} - 0.99 \right]^3 - 10^{-6} \right\} \quad (6)$$

The term $\sum_{f=1}^{20} (P^{f\_comX} \times A^{f\_inner})$ represents the total collagen cross-sectional area that all muscle fibers inserting into the GTO contribute to the X common collagen network. The term abs $(B^{col} \times \sum_{f=1}^{20} T^{f\_comX})^a$ is a damping coefficient for the loosely packed collagen region (scaled to the collagen cross-sectional area); this is a nonlinear function of the force being exerted on the common collagen network (power "a").

OUTPUT OF THE MODEL. The afferent activity in the transduction zone associated with the X common collagen network is obtained by calculating the stretch in its sensory region and scaling it by the appropriate gain factor G (in units of impulses/s $\cdot$ μm^{-2} $\cdot$ stretch^{-1}, where stretch is of unitless dimensions). We assumed that the amount of afferent endings is linearly related to the amount of collagen constituting the common collagen network. The common collagen network with larger collagen cross-sectional area was assumed to have more afferent endings associated with it and to produce greater afferent activity when stretched by length ($L^{comX}_{sens} - L^{com}_{sens\_rest}$) than the common collagen network with smaller collagen cross-sectional area. Thus the common collagen network's afferent firing was modeled as depending on the cross-sectional area of collagen in the X common collagen network and stretch in its sensory region

$$\text{Firing}^{comX} = G \times \sum_{f=1}^{20} (P^{f\_comX} \times A^{f\_inner}) \times (L^{comX}_{sens} - L^{com}_{sens\_rest}) \quad (7)$$

The GTO model afferent output results from the competition between the afferent outputs from the two common collagen networks, which have independent impulse-generating sites. The dominant of the two generator sites wins and produces the output activity of the GTO, suppressing all activity in the weaker generator by resetting it (complete occlusion). The reason for assuming complete rather than partial occlusion is presented in the DISCUSSION.

Construction of the model

The GTO model was designed in the MATLAB Simulink modeling environment. During the design of the Simulink model, certain simplifications had to be introduced in the model because of its complex nature. The complete GTO model contains 64 nonlinear collagen springs and two dampers, so derivation of a single differential equation was very difficult. Therefore we made an assumption that the length of all the collagen that is attached to a fiber inserting into GTO was determined by the fiber's bypassing collagen length. In other words, all the muscle fiber tension is assumed to go into determining the length of the bypassing collagen attached to that fiber. The length of the innervated collagen attached to the same fiber [length of densely packed portion of the fiber's innervated collagen (cross-linking spring) inserting into common collagen network X + length of common collagen network X] is adjusted to equal the fiber's bypassing collagen length. This assumption is a reasonable approximation because the bypassing collagen is much more tightly packed and abundant in the receptor capsule and thus much less compliant than the innervated collagen. The fiber's cross-linking spring that inserts into common network X has much lower stiffness than that of the common network X. Actually, the stiffness of the cross-linking spring represents the fiber's ability to influence activity on the network X's impulse-generating site, which is equal to the stretch of common collagen network X's sensory collagen. When a muscle fiber is being activated, the fiber's cross-linking spring will always experience a larger strain than common collagen network's collagen because it has much lower stiffness than that of the common network X. Once all the fibers in the GTO are tetanically activated, the strain of the common collagen network X and cross-linking springs of all fibers inserting into common collagen network X will be the same because the sum

of the stiffness of all the fibers' cross-linking springs inserting into network X is equal to the stiffness of the common collagen network X.

The GTO model is intended to be applicable to muscles with mixed fiber types in widely varying proportions. The MU composition of a given GTO will vary widely depending on its location in the muscle, so statistical models must be applied to study naturally occurring populations of MUs and GTOs (Mileusnic and Loeb, unpublished observations). For purposes of validating the generic properties of the GTO model, we composed an "average GTO" that received input from five S, four FR, and four FF MUs. The larger number of type S MUs reflects the tendency of GTOs to be more common in the deep portions of mixed muscles such as the feline MG (Burke and Tsairis 1973), from which most GTO physiological data have been derived. We assumed that each MU has an average of 1.6 muscle fibers inserting into the GTO (Gregory 1990). Therefore the "average GTO model" consisted of 13 MUs (five S, four FR, and four FF) and 20.8 muscle fibers. The GTO's innervated collagen was assumed to be evenly distributed between two common collagen networks. The same was assumed for the individual fiber's innervated collagen. Note that for the "average GTO model" the summation terms over 20 muscle fibers [$\sum_{f=1}^{20} T^{f\_comX}$, $\sum_{f=1}^{20} (P^{f\_comX} \times A^{f\_inner})$, and abs $(B^{col} \times \sum_{f=1}^{20} T^{f\_comX})^a$] in *Eqs. 5*, *6*, and *7* were replaced by the summation terms over 13 MUs [$\sum_{f=1}^{13} T^{f\_comX}$, $\sum_{f=1}^{13} (P^{f\_comX} \times A^{f\_inner})$, and abs $(B^{col} \times \sum_{f=1}^{13} T^{f\_comX})^a$] because 1.6 fibers per each MU were assumed to insert into GTO. Therefore the parameter values listed in Table 1 are per 1.6 fibers and not per single fiber as for the other models.

The "average GTO model" with 1.6 fibers/MU is, of course, not possible, so we developed a "realistic GTO model" where each MU was allowed to have either one or two fibers in series with the receptor. The realistic GTO model had 13 MUs: three S MUs had two inserting fibers, two S MUs had one fiber, and half of the four FR and four FF MUs contributed two fibers whereas the others had one. The total number of muscle fibers inserting into the GTO was thus 20. The GTO's loosely packed collagen was assumed to be evenly distributed between two common collagen networks. The parameter values that were used for the case of the realistic GTO model are listed in Table 1.

Finally, two additional GTO models were designed to accommodate the different fiber composition or muscle of origin of various GTOs whose activity we sought to reproduce in our models. For more details see RESULTS and Table 1.

Parameter determination

The model parameters were manually tuned to fit the experimental data capturing the GTO afferent response (Gregory and Proske 1979), within limits suggested by the available histology and morphometry. Parameter optimization (such as used in our model of the muscle spindle; Mileusnic et al. 2006) was not used in this study because the available experimental data are sparse and highly variable, particularly for the more complex aspects of GTO behavior (such as cross-adaptation and nonlinear summation). The experimental records that were used in our modeling will be discussed in greater detail in RESULTS (see *Dynamic and static responses* and *Nonlinear summation*).

The rest lengths of nonlinear collagen springs within the model had unitless dimensions. For simplicity, we assumed that the rest length of the whole system (L_{rest}^{bypass}) is equal to 1 and then distributed the lengths of individual components in the model in a way that was anatomically realistic and produced physiologically realistic behavior. Parameters were constrained to keep all component springs operating within the 4–5% strain measured experimentally (maximal physiological strain of tendon and aponeurosis is roughly 4–5% of its slack length; Brown et al. 1996; Scott and Loeb 1995). This was particularly challenging during the activation of the first muscle fiber in the GTO because its densely packed portion of innervated collagen that inserts into common collagen network has significantly lower stiffness than that of the common collagen network. Because the common collagen network is not stretched by any other fibers inserting into the GTO, the first fiber's densely packed portion of innervated collagen needs to be extensively stretched for the summation of common collagen network's length and the length of the first fiber's densely packed portion of innervated collagen to equal the fiber's bypassing collagen length. Therefore to keep the stretch of all elements within the physiological range, we assumed that the stretch of the whole GTO during tetanic contraction of all inserting muscle fibers is around 2.5%. Although this value is somewhat lower than the maximal stretch that was measured in a typical tendon, it agrees well with experimental observations in which the GTO was found to have a larger Young's modulus than that of tendon (Fukami and Wilkinson 1977). The rest lengths of the common collagen network's sensory region ($L_{sens\_rest}^{com}$), loosely packed collagen region ($L_{loose\_rest}^{com}$), and fiber's densely packed portion of innervated collagen ($L_{rest}^{bypass} - L_{loose\_rest}^{com} - L_{sens\_rest}^{com}$) that were found to produce the best results are shown in Table 2.

The collagen stress–strain relationship that we used (*Eq. 2*) differs slightly from the one suggested by Brown and Scott (Scott and Loeb

TABLE 1. *GTO cross-sectional area model parameters*

Parameter	Description	S	FR	FF
θ^f	The fibers petal angle (rad)	0.426, 0.278, 0.254, 0.242	0.467, 0.305, _, _	0.570, 0.372, 0.340, _
r^f	The radius of the fiber's lattice (μm)	119, 117, 122, 176	131, 128, _, _	160, 157, 164, _
A^f	The total fiber's cross-sectional area (μm^2)	3032, 1895, 1895, 3738	4013, 2508, _, _	7288, 4555, 4555, _
A^{f_inner}	The area of the fiber's innervated collagen (μm^2)	408, 254, 303, 374	449, 279, _, _	548, 341, 407, _
A^{f_bypass}	The area of the fiber's bypassing collagen (μm^2)	2624, 1641, 1592, 3364	3564, 2229, _, _	6740, 4214, 4148, _
P^{f_com1}	The percentage of fiber's innervated collagen that contributes to the common collagen network #1	$0 \le P^{f\_com1} \le 1$	$0 \le P^{f\_com1} \le 1$	$0 \le P^{f\_com1} \le 1$
P^{f_com2}	The percentage of fiber's innervated collagen that contributes to the common collagen network #2	$1 - P^{f\_com1}$	$1 - P^{f\_com1}$	$1 - P^{f\_com1}$

The GTO's cross-sectional area values for the "average GTO model" (composed of 20.8 fibers organized in five S, four FR, and four FF), "realistic GTO model" (composed of 20 fibers organized in five S, four FR, and four FF MUs), GTO model used to obtain Fig. 5*A* (composed of 20 fibers organized in eight FF and six S MUs), and soleus GTO (composed of 26 fibers organized in 22 S MUs) are presented in that order in each column. The values given are for a single fiber, whereas in the "average GTO model" they are for 1.6 fibers. For all models, it was assumed that the 10% of total GTO area is occupied by the innervated collagen type. The total cross-sectional areas originate from the experimentally obtained measurements (Burke 1981).

TABLE 2. *GTO model parameters for MG muscle*

Parameter	Description	S	FR	FF
K^{col}	Collagen coefficient per collagen cross-sectional area [N/μm^2]	0.0083	0.0083	0.0083
B^{col}	Damping coefficient per collagen cross-sectional area [l/μm^2]	$1.47 * 10^{-4}$	$1.47 * 10^{-4}$	$1.47 * 10^{-4}$
G	Gain relating the sensory region stretch to gen. potential [(imp(s)/μm^2]	44.2	44.2	44.2
a	Nonlinear force dependence coefficient of damping term [unitless]	0.4	0.4	0.4
$L_{rest}^{f\_bypass}$	Bypassing collagen rest length [unitless]	1	1	1
$L_{sens\_rest}^{com}$	Common collagen network sensory region rest length [unitless]	0.01	0.01	0.01
$L_{loose\_rest}^{com}$	Common loosely packed collagen network rest length [unitless]	0.44	0.44	0.44

1995). We preferred *Eq. 2* because of the presence of some terms in Brown and Scott's equation that were undefined for certain values (for example, natural log of zero). The collagen-related constant (K^{col}) was estimated based on the experimentally measured tendon's force–length curve (Brown et al. 1996; Scott and Loeb 1995). The damping coefficient per collagen cross-sectional area (B^{col}) was estimated by using the MG's GTO record obtained during the tetanic activation of eight MUs (although the particular MUs were not identified as FF, we decided they were FF type based on their tension-producing ability; see Fig. 2 in Gregory and Proske 1979). By testing our model's ability to reproduce these records, it was revealed that our initial assumption involving a constant damping coefficient was inappropriate. We achieved a much better fit by incorporating a damping coefficient that depended nonlinearly on the force applied to the loosely packed common collagen, such as might be expected if the packing density and viscous flow among these elements were modified by this force. The best results were obtained when power term "a" (see *Eq. 6*) was set to 0.4. Finally, the constant relating the sensory region stretch to the generator potential (G) was adjusted to match measurements reported by Gregory and Proske (1979) of GTO afferent response (67 pps) at 0.5 s during steady tetanic stimulation of an FF MU (see *Dynamic and static responses* in RESULTS). We decided to use a single gain parameter for all three types of muscle fibers and to explain their ability to produce different afferent firing through their ability to distort impulse-generating sites at common collagen networks, and thus through the collagen's nonlinear stress–strain properties.

The last set of parameters that needed to be determined was the distribution of collagen from each muscle fiber into bypassing and innervated types. We designed a conceptual geometrical arrangement of fibers inserting into the GTO (see Fig. 2*B*) where the GTO's cross-sectional area was assumed to be flower shaped and the fibers were arranged in the manner of flower petals. The cumulative innervated collagen belonging to all the muscle fibers inserting into the GTO was assumed to occupy an inner zone (10% of the total GTO collagen) of the flower-shaped cross-sectional area. We identified a simple scaling rule for the shapes of the petals that produced the nonlinear scaling of GTO responses to contractions of muscle fibers with different cross-sectional areas (see the APPENDIX). This type of fiber arrangement enabled the model to capture the relatively similar static and dynamic responses during the tetanic activation of three types of muscle fibers despite the very different amounts of collagen contributed by each [fiber cross-sectional areas: 1,895 (S), 2,504 (FR), and 4,555 μm^2 (FF); Burke 1981] and the different tensions they exert [fiber tetanic tensions: 0.606 (S), 0.801 (FR), and 1.454 mN (FF); estimated using the specific tension of 32 N/cm^2 (Scott et al. 1996)].

RESULTS

Most GTO experiments in the literature were performed on feline soleus or MG muscle. We chose MG because it is a heterogeneous muscle and it was of interest to study how fibers of different types influence the GTO afferent response. The literature describes the GTO afferent behavior in a qualitative sense but there are relatively few quantitative records of GTO responses to type-identified MUs. In the following subsections we compare modeled and quantitative experimental behavior under *Dynamic and static responses* and *Nonlinear summation* and some qualitative experimental observations regarding *Self- and cross-adaptation* and *The relationship between cross-adaptation and summation*.

Dynamic and static responses

The model's prediction of the GTO afferent response (dynamic and static responses) during tetanic activation of MUs composed of three types of muscle fibers (S: . . ., FR: —, FF: - - -) is shown in Fig. 3*A*. To obtain these measurements we used the "average GTO model" where a MU on average contributed 1.6 fibers to GTO and where each MU's innervated

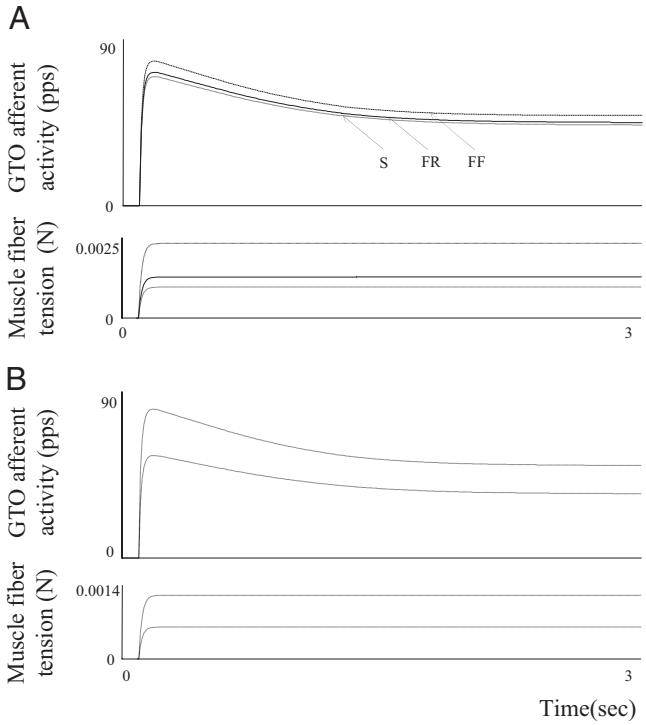

FIG. 3. GTO model response during tetanic activation of motor units (MUs). *A*: response of "average GTO model" during tetanic activation of 3 types of MUs (S: . . ., FR: —; and FF: - - -), each having a single muscle fiber inserting into the receptor. Fiber's innervated collagen is assumed to be evenly distributed between the 2 common collagen networks. Model demonstrates the experimentally observed dynamic and static GTO afferent response. *B*: response of "realistic GTO model" during tetanic stimulation of S MU, which had either one (smaller GTO response) or 2 (larger GTO response) of its fibers inserting into the GTO. Innervated collagen is assumed to be evenly distributed between the 2 common collagen networks.

collagen was evenly distributed between two common collagen networks (in other words $P^{f\_com1} = 0.5$ and $P^{f\_com2} = 0.5$). Because the static and dynamic responses were never explicitly experimentally measured for different types of MUs in the cat's MG GTO, we had to rely on the experimental measurement of the GTO afferent responses after 0.5 s of the maintained tetanic stimulation of three types of MUs that captured static but also traces of the dynamic GTO response. The model's prediction of the GTO afferent responses at 0.5 s during the maintained tetanic stimulation of MUs were 60.4 pps for type S, 62.3 pps for type FR and 67 pps for type FF MUs; the experimental literature measured 56 (S), 55 (FR), and 67 pps (FF) (Gregory and Proske 1979). Our model's ability to capture comparable GTO responses for three types of muscle fibers despite the very different tensions they exert on the GTO lies in the GTO's flower-shaped cross-sectional area plus a simple scaling rule for different size petals (see the APPENDIX).

The decay time of the GTO's dynamic response has never been measured directly. Instead, we used the MG GTO record obtained during the tetanic activation of a progressively larger number of MUs (eight FF MUs; see Fig. 2 in Gregory and Proske 1979) to estimate the damping coefficient per collagen cross-sectional area and dynamic response decay time. The dynamic response decay times predicted by the model to some 10% of peak value after the tetanic activation of S, FR, and FF MUs (each having 1.6 fibers inserting into capsule) were 1.475, 1.464, and 1.433 s, respectively.

Because a typical MU contributes one or two fibers into the GTO rather than 1.6 fibers, a large variability among GTO responses to tetanic activation of different MUs can be expected and has been reported in the literature. For example, the measured SDs for the average GTO responses after 0.5 s of tetanic activation of three types of MUs were ±20 (S), ±27 (FR), and ±32 pps (FF) (Gregory and Proske 1979). The "realistic GTO model" demonstrated such variability when we compared the predicted GTO response during tetanic activation of two S MUs, one contributing one fiber and the other contributing two fibers to the GTO (Fig. 3*B*).

Self- and cross-adaptation

The model's ability to capture self- and cross-adaptation was studied by using the "realistic GTO model" because the average experimental measurements of such phenomena were not available (Fig. 4). In Fig. 4*A*, the self-adaptation property is demonstrated for three types of MUs (S: . . .; FR: —; and FF: - - -), each contributing a single fiber into the receptor capsule and whose innervated collagen was evenly distributed between two common collagen networks. To study the self-adaptation, the "realistic GTO model" was first presented with the tetanic MU activation for 2 s. The activation was then removed and reapplied to the same MU 0.5 s afterward. The ability of our model to capture this GTO phenomenon lies in the loosely packed collagen, whose viscosity causes it to rearrange itself and recover its original length only gradually.

To demonstrate cross-adaptation, the same temporal pattern of muscle fiber activation was applied but with each burst of activation directed to a different muscle fiber. Figure 4*B* demonstrates this property for the case of two FF MUs where each had a single fiber inserting into the receptor. The experimental literature describes large variability in the amount of cross-adaptation that exists between different MUs (Gregory et al. 1985). To demonstrate such variability, we adjusted the model parameters so that the muscle fibers no longer contributed equally to each common collagen network. In one MU pair, the first MU's fiber had 90% of its innervated collagen in the first common collagen network and 10% in the second

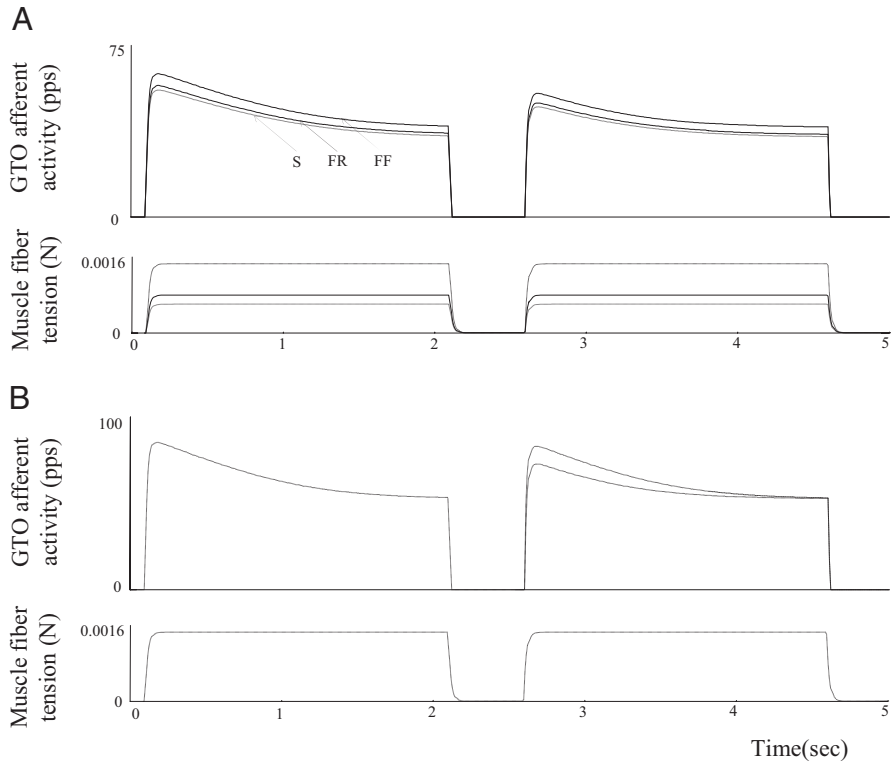

FIG. 4. Model's ability to capture self- and cross-adaptation. *A*: ability of "realistic GTO model" to capture the self-adaptation for 3 types of MUs (S: . . ., FR: —; and FF: — - -). Self-adaptation was obtained by initially presenting the model with the abrupt MU's tension increase, which was then removed and reapplied 0.5 s afterward. It was assumed that each MU had one fiber inserting into the GTO and its innervated collagen was equally divided between 2 common collagen networks. *B*: ability of "realistic GTO model" to capture cross-adaptation. In this example 2 FF MUs each having a single muscle fiber inserting into the GTO were used. Cross-adaptation was obtained by driving the model with a 2-s-long force step produced by the first MU, then a 0.5-s pause and a similar force step produced by the second MU. In one example, the first MU's fiber had 90% of its innervated collagen in the first common collagen network and 10% in the second common collagen network, whereas the second MU's fiber had the opposite. This arrangement resulted in very little cross-adaptation (larger second peak). When we assumed that both MUs' fibers had 90% of their innervated collagen in the first common collagen network and 10% in the second common collagen network, the cross-adaptation was much stronger (smaller second peak).

common collagen network, whereas the second MU's fiber had the opposite. This arrangement resulted in very little cross-adaptation (Fig. 4*B*, larger second peak). When we assumed that both MUs' fibers had 90% of their innervated collagen in the first common collagen network and 10% in the second common collagen network, the cross-adaptation was much stronger (Fig. 4*B*, smaller second peak). Thus the cross-adaptation between two MUs reflects the degree to which their inputs to the two common collagen networks are distributed similarly.

Nonlinear summation

During the activation of multiple MUs the GTO demonstrates nonlinear summation, where two MUs when stimulated simultaneously produce afferent activity that is smaller than the linear summation of the GTO firing rates that individual MUs produce when stimulated independently. Figure 5*A* shows the experimentally recorded MG's GTO afferent activity to progressively larger numbers of MUs (Gregory and Proske 1979). Based on the tension record provided in the experiments, we assumed that all eight MUs were of FF muscle fiber type. To test our model's ability to capture these experimental data, we designed an additional GTO model having a fiber composition different from that of the previously used GTO model. The new model consisted of eight FF MUs (six having two fibers and two having one fiber inserting into GTO) and five S MUs (two having two fibers and three having one fiber inserting into GTO) and had their innervated collagen evenly distributed between two common collagen networks. Assigning the number of fibers each MU contributes to the GTO was performed in a manner that produced the best fit between experimental records and the model's GTO afferent prediction (first FF MU: two fibers; second FF MU: one fiber; third FF MU: two fibers; fourth FF MU: two fibers; fifth FF MU: two fibers; sixth FF MU: two fibers; seventh FF MU: two fibers; eighth FF MU: one fiber). The model's predictions are presented along the experimental data and demonstrate the model's ability to accurately capture the nonlinear summation of static responses and the dynamic responses (except for initial, brief transients that may reflect unphysiological synchronization of recruited MUs).

Figure 5*B* represents another example of the nonlinear summation where all 13 MUs inserting into the "realistic GTO model" were activated one after the other in the order similar to that found in natural recruitment where all S MUs are activated first, followed by FR MUs and then FF MUs. The MUs were activated in the following order: S (1), S (2), S (1), S (2), S (2), FR (1), FR (2), FR (1), FR (2), FF (1), FF (2), FF (1), and FF (2), where the numbers in parentheses represent the number of fibers each MU contributed to the GTO. In natural recruitment, the tension produced by each successively recruited MU would increase gradually during the recruitment of subsequent units because its firing rate would be modulated as well. This example assumes stepwise recruitment of each successive MU at a single frequency sufficient to produce a fused contraction, which is the usual experimental paradigm when using electrical stimulation of MUs. The model prediction is qualitatively similar to the recorded response of the biological GTO to a progressively larger number of MUs where addition of each successive MU has progressively diminished effects on the total GTO response (Crago et al. 1982;

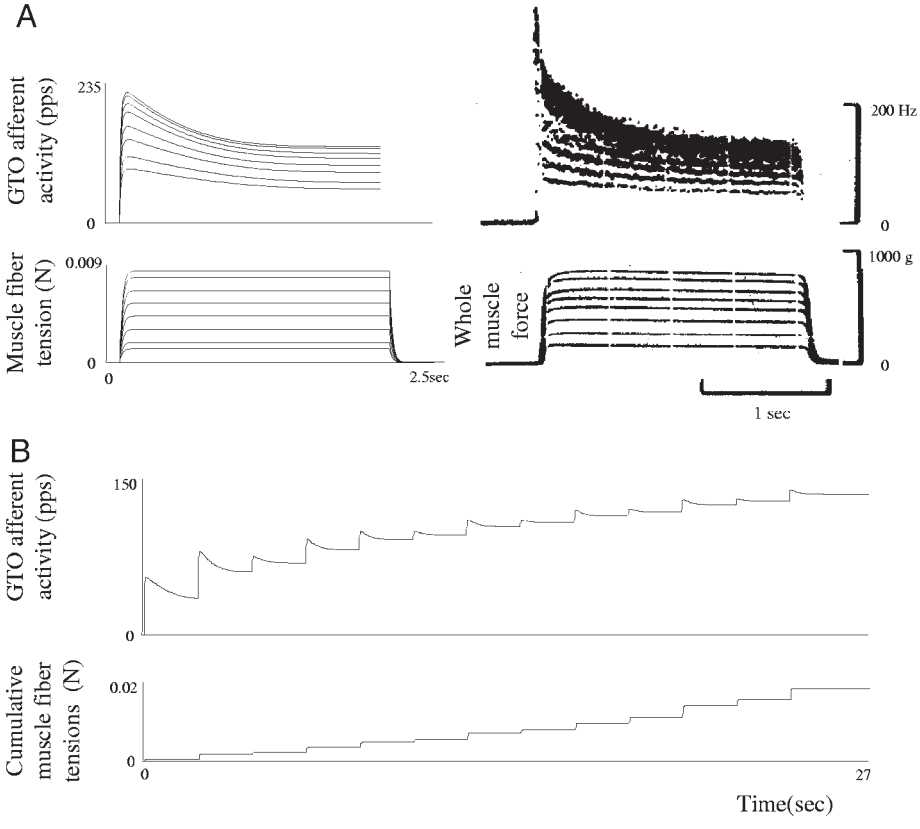

FIG. 5. Model's ability to capture nonlinear summation. *A*: MG's GTO afferent activity in response to progressive recruitment of 8 MUs. GTO model consisted of 8 FF MUs (6 having 2 fibers and 2 having one fiber inserting into GTO) and 5 S MUs (2 having 2 fibers and 3 having one fiber inserting into GTO). All MUs were assumed to have their innervated collagen evenly distributed between 2 common collagen networks. Assigning the number of fibers each MU contributes to the GTO was performed in a manner that produced the best fit between experimental records (Gregory and Proske 1979) and model's GTO afferent prediction (1st FF MU: 2 fibers; 2nd FF MU: 1 fibers; 3rd FF MU: 2 fiber; 4th FF MU: 2 fibers; 5th FF MU: 2 fibers; 6th FF MU: 2 fibers; 7th FF MU: 2 fibers; 8th FF MU: 1 fiber). *B*: response of "realistic GTO model" to tension developed by stimulation of progressively larger number of MUs. All 13 MUs inserting into the "realistic GTO model" were activated one after the other in the order similar to that found in natural recruitment where all S MUs are activated before FR MUs and where FF MUs are the last to be activated. MUs were activated in the following order: S (1), S (2), S (1), S (2), S (2), FR (1), FR (2), FR (1), FR (2), FF (1), FF (2), FF (1), and FF (2), where the numbers in parentheses represent the number of fibers MU contributed to the GTO. Cumulative GTO response and cumulative tensions of all muscle fibers are shown.

Gregory and Proske 1979; Proske and Gregory 1980). Whereas the tension experienced by the GTO rises gradually with the addition of each activated MU, the GTO afferent activity rises abruptly and then plateaus long before tension levels out. The dynamic peaks caused by the activation of each additional MU are visible and similar to those reported in the biological system where they are described as the "beating effect" (Crago et al. 1982).

The model's ability to capture nonlinear summation during the activation of multiple MUs is the result of two design features. The nonlinear property of the collagen's stress–strain relationship is an obvious contributor, but if it were the only factor, it could not account for the variability of such nonlinear summation. The second source of nonlinearity involves the existence of multiple impulse-generating sites in the GTO. Two MUs having their innervated collagen regions located at separate transduction sites will produce very low (or no) summation during simultaneous activation because the afferent activity will be dominated by whichever transduction site has the highest firing rate. There will be no effect from tension in the other transduction site unless and until it becomes dominant. If they contribute similarly to the common transduction sites, then the nonlinear properties of the collagen result in a high degree of nonlinear summation in the afferent activity that actually emerges from the GTO. Extensive attempts to reproduce this effect with GTO models having only one transduction site were unsuccessful.

The relationship between the cross-adaptation and summation

Assuming the existence of multiple impulse-generating sites was also crucial in the model's ability to capture the quantitative relationship between the cross-adaptation and summation between two MUs inserting their fibers into the GTO.

In experiments by Gregory et al. (1985) pairs of MUs that produced comparable responses in a single GTO (difference $<10\%$) when individually stimulated tetanically were identified in the cat soleus muscle. The pairs were used to study cross-adaptation and summation quantitatively. In studying the cross-adaptation, MU "B" was tetanically stimulated for 2 s, followed by a 0.5-s pause and then stimulation of MU "A" tetanically for 2 s. The cross-adaptation was defined as the difference in the mean afferent activity during the first 0.5 s after the beginning of the tetanic stimulation of MU B minus A. The cross-adaptation was then normalized by the self-adaptation of MU A (obtained in the same manner as the cross-adaptation except that both tetanic trains were delivered to MU A). The summation coefficient for the paired MUs was estimated as the percentage of GTO response generated by the MU producing the smaller response, which adds to the GTO response generated by the MU producing the larger GTO response to obtain the cumulative response

$$\text{Summation coefficient} = \frac{\text{Cumulative response} - \text{GTO response of MU producing larger response}}{\text{GTO response of MU producing smaller response}}$$

To replicate this experiment with our model, several modifications had to be introduced in the model to account for the differences between the MG and soleus GTOs. In particular, it was necessary to account for the average of 26 muscle fibers of the same type (S) that insert into the soleus GTO in comparison to 20 fibers of three different types that insert into MG's GTO (Spielmann and Stauffer 1986). By arranging the fibers in the flower-shaped pattern (see the APPENDIX), we estimated that each fiber in the soleus GTO occupied some $2\pi/26$ radians of the total innervated collagen circular area. The literature suggests that these 26 fibers typically originate from 22 MUs, where each MU contributes some 1.22 muscle fibers to the soleus' GTO (Spielmann and Stauffer 1986). Rather than using the average number of muscle fibers per MU in our model, we assumed that 18 MUs had one and four MUs had two muscle fibers inserting into the receptor. We assumed that the innervated collagen occupied 10% of the innermost area of the GTO, whereas the gain factor (G; in units of impulses/s $\cdot$ μm^{-2} $\cdot$ stretch^{-1}) was assumed to be the same as for the MG's GTO (see Table 1).

In modeling the relationship between the summation and cross-adaptation coefficients (Fig. 6), we first compared the MU pairs that each had a single fiber inserting into the GTO and that produced the identical GTO responses. We systematically varied the similarity of their contributions to two com-

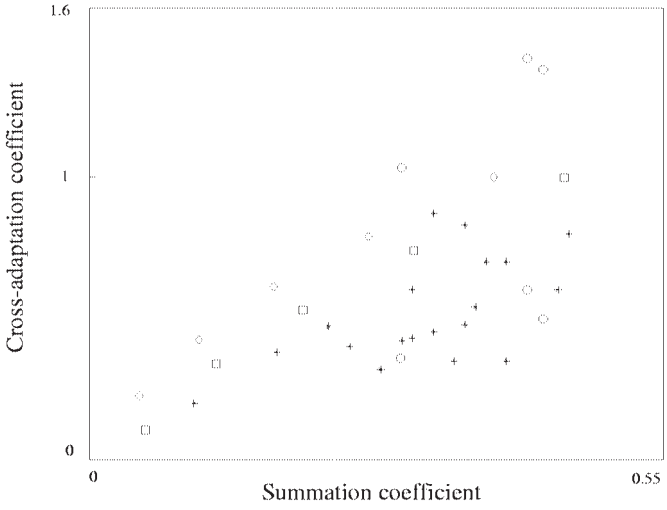

FIG. 6. Relationship between the cross-adaptation and summation. "Realistic GTO model" was modified to capture the properties of the feline soleus GTO (see text) from which the available experimental data originate (parameter values are listed in Table 1). Cross-adaptation is defined as the difference in the mean afferent activity (measured during the first 0.5 s of the tetanic stimulation) between the GTO response to the "B" MU and to the "A" MU activation. Cross-adaptation was normalized by the "A" MU's self-adaptation (obtained in the same manner as the cross-adaptation except that first stimulation involved the "A" rather than the "B" MU) to obtain the cross-adaptation coefficient. Afterward, the summation amount for the paired MUs was obtained by calculating the percentage of the smaller MU's response that adds to the larger MU's response to obtain the cumulative response when 2 MUs were stimulated simultaneously. Experimental data are shown as * for comparison with the model predictions for pairs of MUs where relative contributions to the 2 transduction zones ranged from 10 to 90% overlap. □: denotes MU pairs producing exactly the same GTO responses where each had a single fiber inserting into the GTO; ◇: denotes MU pairs producing exactly the same GTO responses where each had 2 fibers inserting into the GTO. ○: denotes the model predictions for 2 MUs each contributing a single fiber to the GTO but with 10% difference in their individual effects on afferent firing (see text).

mon collagen networks between 0.9 and 0.5 while keeping the other parameters constant:

- Case 1:
  MU A ($P^{f\_com1} = 0.9$, $P^{f\_com2} = 0.1$) vs. MU B ($P^{f\_com1} = 0.1$, $P^{f\_com2} = 0.9$)
- Case 2:
  MU A ($P^{f\_com1} = 0.8$, $P^{f\_com2} = 0.2$) vs. MU B ($P^{f\_com1} = 0.2$, $P^{f\_com2} = 0.8$)
- Case 3:
  MU A ($P^{f\_com1} = 0.7$, $P^{f\_com2} = 0.3$) vs. MU B ($P^{f\_com1} = 0.3$, $P^{f\_com2} = 0.7$)
- Case 4:
  MU A ($P^{f\_com1} = 0.6$, $P^{f\_com2} = 0.4$) vs. MU B ($P^{f\_com1} = 0.4$, $P^{f\_com2} = 0.6$)
- Case 5:
  MU A ($P^{f\_com1} = 0.5$, $P^{f\_com2} = 0.5$) vs. MU B ($P^{f\_com1} = 0.5$, $P^{f\_com2} = 0.5$)

Low degrees of overlap (e.g., Case 1) produced both low summation and low cross-adaptation. High degrees of overlap produced both high summation and high cross-adaptation; overlap even higher than Case 5 had the same cross-adaptation and only slightly higher summation than Case 5. A similar comparison was repeated for the MU pairs having the same GTO responses while contributing two fibers each to the GTO. In addition to studying MU pairs that produced the identical GTO responses, we decided to compare MUs whose individual effects were different but within the 10% criterion of Gregory et al. These seemingly minor changes had interesting effects. When a MU was conditioned by another MU that had a slightly lower GTO response, the cross-adaptation coefficient and summation coefficient values fell among those measured in Gregory's experiments. However, when the MU was conditioned by the MU that produced a slightly larger GTO response, the cross-adaptation coefficient values were typically greater than unity. Such cross-adaptation coefficient values were not plotted in Gregory's data and will be discussed in more detail in the DISCUSSION section.

Incorporating multiple impulse-generating sites was necessary for the model to capture the proportional relationship between the cross-adaptation and summation. In the GTO model with only a single impulse-generating site, afferent activity resulted from the summation of depolarizing current from different afferent branches. In this case, the two MUs produced the largest cumulative response when they inserted onto common collagen networks innervated by separate afferent branches. This arrangement, however, resulted in very low cross-adaptation between two MUs and contradicted the experimental observations. A model consisting of two impulse-generating sites, however, predicted the proportional relationship between these two quantities. We would expect, but have not explicitly tested, that similar results could be obtained from models with more than two generators.

DISCUSSION

Based on the response of GTO afferents to passive tension, the GTO was once considered as a protective organ that discharged only at high muscle tensions. The GTO's role was reevaluated when it was demonstrated to be capable of monitoring active muscle tension over a much wider range than initially thought (Alneas 1967; Crago et al. 1982; Horcholle-Bossavit et al. 1990; Houk and Henneman 1967). Our goal was to develop a physiologically realistic model that consisted of anatomical components found in the biological GTO and whose properties were described in the experimental literature (e.g., nonlinear springlike properties of collagen). We are pleased that a relatively simple and anatomically realistic model is capable of describing many complexities of the GTO response that have puzzled researchers over many years.

Static and dynamic responses during the tetanic contractions of different types of muscle fibers are captured well by the model. The experimental literature suggests that the average GTO responses after 0.5 s of sustained MU tetanic stimulation are 56 (S), 55 (FR), and 67 pps (FF) (Gregory and Proske 1979), whereas our model predicts 60.4 (S), 62.3 (FR), and 67 pps (FF). There are several reasons to expect small discrepancies, including variability in the design and experimental sampling of the GTOs themselves. Other factors include our assumption that stretch of the sensory region's collagen is linearly related to the sensory ending stretch alone, with no velocity component. This assumption was made for simplicity but might not be exactly true in the biological system. Additionally, it is possible that the discrepancy reflects the difference between the estimated collagen stress–strain relationship and the actual relationship, or perhaps a difference in packing property of tendinous versus GTO collagen. The third potential source of discrepancy is the cross-sectional model of the GTO, especially the scaling rule for the shapes of petals. The model's current scaling rule for petals maintains a constant ratio between the petal radius and angle (r/θ) for different sizes of petals, which is appealingly simple but arbitrary (see following text and the APPENDIX). Finally, it is possible that on average a single FF MU contributes slightly more that 1.6 fibers to each GTO and S and FR MUs on average <1.6 fibers, which is explained by the fact that in MG there are more FF muscle fibers. This would result in larger differences in the GTO firing among the three types of MUs than predicted by our model.

The model's ability to capture the nonlinear summation of afferent activity when multiple MUs are active simultaneously is shown in Fig. 5*A*. The nonlinear summation of static responses is captured accurately, especially during the activation of the first four MUs, whereas during the addition of four remaining MUs it slightly underestimates the recorded afferent activity. The same is true for the dynamic response, where the first four MU responses are captured more accurately than those produced by later recruited MUs. It is possible that the very large dynamic response (about 200 pps for the case where eight MUs are simultaneously activated) may approach a saturation nonlinearity in the impulse-generating site that presumably exists in the biological GTO.

Self- and cross-adaptation during activation of multiple muscle fibers inserting into a GTO are well reproduced by the model, as well as the proportional relationship between the nonlinear summation and cross-adaptation that was reported in the literature. When the MU pairs producing the identical GTO afferent activity are compared, the cross-adaptation and summation coefficients are very close to the experimental observations. Comparison of MU pairs that produced slightly different GTO activity ($<10\%$) but within the range treated as equal in experiments by Gregory et al. (1985), however, provided some interesting new observations, particularly for the case of cross-adaptation coefficient values greater than unity. Gregory et al. (1985) actually mention obtaining cross-adaptation coefficient values larger than unity when the time between two stimulations was 1 s rather than 0.5 s, but they

suggested that such observations were artifactual and unreliable. Our model demonstrates that cross-adaptation coefficient values greater than unity are possible for both the 0.5- and 1-s cases when the MU producing the weaker GTO response is being conditioned (proceeded) by the MU producing the larger GTO response (difference $<10\%$). Gregory and Proske (1981) did provide experimental examples where cross-adaptation was observed to be larger than self-adaptation (meaning the cross-adaptation coefficient was greater than unity), that is, when the conditioning MU had a larger GTO response than that of the conditioned MU. In those observations the two fibers being compared produced very different afferent firing rates; nevertheless, they confirm our prediction that cross-adaptation coefficient values can exceed unity. We are unsure why the data from Gregory et al. (1985) do not demonstrate this phenomenon. Based on their recollection (U. Proske, personal communication), they suggest that no preference was given to conditioning the MU by the MU producing the (slightly) smaller GTO response. However, if one considers their definition of

$$\text{Summation coefficient} = \frac{\text{Cumulative response} - \text{GTO response of MU producing larger response}}{\text{GTO response of MU producing smaller response}}$$

and the fact that they studied the percentage of the smaller GTO response that adds to the larger one, then it would also be reasonable that they had studied the weaker MU's ability to cross-adapt the other MU having larger GTO response.

The flower-shaped model of the GTO's cross-sectional area, as mentioned earlier, is not grounded on any explicit experimental observations. However, there must exist some type of structured system and apportioning mechanism so that every fiber contributes a nonrandom percentage of its myotendinous collagen to the innervated region of the GTO that can influence afferent activity. Additionally, the fiber's innervated collagen contribution is not simply proportional to its size; S muscle fibers are systematically overrepresented in comparison to the larger FR and FF muscle fibers. Some observations suggest that smaller S fibers tend to be located in the middle of each muscle fascicle and insert into the GTO at the central area, whereas the larger FR and FF fibers insert more circumferentially across the GTO's muscle end (Richmond 1974). This observation perhaps explains why the S fibers are overrepresented because innervated collagen is typically found more centrally within the receptor capsule. However, there are data from the cat's soleus muscle (homogeneous slow fiber type) that suggest that a muscle fiber's ability to excite the GTO is independent of its insertion location at the muscle end, arguing against a simple anatomical explanation (Spielmann and Stauffer 1986). Our flower-shaped model of the GTO's cross-sectional structure is conceptual and does not imply that such a structure should be visualizable histologically. Furthermore, our model represents average physiological properties for a structure that is known to have relatively high variability.

Impulse-generating sites

Currently, there is no direct experimental evidence supporting the existence of multiple impulse-generating sites (see Jami 1992). The large myelinated branches typically found in the receptor capsule (Nitatori 1988; Schoultz and Swett 1973), however, would be consistent with the multiple generators identified in cutaneous afferents (Goldfinger and Fukami 1981) and suggested for muscle spindle primary afferents (see companion paper by Mileusnic et al. 2006). Although unmyelinated sensory terminals are thought to generate only receptor potentials, myelinated fibers serve to conduct action potentials and, theoretically, initiation of impulses can be expected to occur at or near the first node of Ranvier, although this is not necessarily true; in some frog muscle spindles impulses can be generated at one terminal node and not at the other (Ito et al. 1974). Additional indirect evidence supporting the existence of two (or more) impulse-generating sites in the GTO originates from studies looking at the ability of muscle fibers inserting into the GTO along the capsule rather than at the muscle end to excite the receptor. If the GTO activity originated from a single impulse-generating site, then one would expect that the closer the fiber inserts to the GTO's muscle end, the greater would be its ability to excite the GTO. Interestingly, some limited evidence suggests that fibers inserting into the capsule at least halfway along the GTO still have a robust effect on the GTO afferent firing comparable to that of those inserting at the muscle end (Spielmann and Stauffer 1986). If GTO activity results from the competition between two (or more) impulse-generating sites, then the muscle fiber bypassing the first site will still be capable of influencing the second one and generating GTO activity comparable to that produced by a muscle fiber inserting at the muscle end of the capsule (but only if there is a mechanism to ensure that the bypassing fiber has the usual proportional termination on the loosely packed collagen deep in the capsule as described before). Finally, our model together with another modeling study (Gregory et al. 1985) suggest that assuming multiple generating sites is crucial to capturing the complex GTO behavior, particularly the nonlinear summation and the proportional relationship between the nonlinear summation and cross-adaptation.

If we assume that multiple generating sites exist in a single GTO, it still remains unknown how many such sites might be present. We chose to use two such sites in our model because the literature suggests the existence of typically two large myelinated branches in the GTO capsule. It is possible that GTO activity results from more than two branches as some researchers suggested (Gregory and Proske 1981; see *Comparison with previous modeling attempts*).

Finally, our model assumed complete rather than partial occlusion between two impulse-generating sites. The activity of muscle spindle primary afferents is most consistent with partial occlusion (Banks et al. 1997; Carr et al. 1998; Fallon et al. 2001; as modeled in Mileusnic et al. 2006). No data for the GTO suggest partial inclusion and our model performed well with the simpler assumption of complete occlusion.

Unloading of GTO by contraction of in-parallel muscle fibers

The effect of unloading of the GTO (reduction of its afferent firing) by contraction of in-parallel muscle fibers was not incorporated in our model. The experimental literature on this phenomenon is highly variable and inconclusive. In 1967 Houk and Henneman first reported this effect in the cat's soleus muscle where they noticed it only when the GTO was passively stretched and not during MU activation (Houk and Henneman

1967). Opposite conclusions were reached by different researchers who found that activation of some of the muscle's MUs can reduce afferent firing (Binder 1981; Stuart et al. 1972). Further studies on the in-parallel fiber unloading concluded that in soleus muscle in-parallel unloading contractions did not reduce the response of a GTO to an activating MU unless the muscle was held in the initial, steep portion of its length–tension relationship (Gregory et al. 1986). This suggested that the contraction of the unloading MUs and stretch of in-series connective tissue might produce some internal shortening within the muscle, thereby lowering active tension in muscle fibers pulling directly on the receptor (Proske 1993).

Tension in muscle fibers running in parallel with the receptor and inserting into the whole-muscle aponeurosis or tendon near the insertion of the tendon organ may affect the deformation of the intracapsular collagenous fascicles in response to the contraction of the muscle fibers actually inserting into the GTO (Horcholle-Bossavit et al. 1990). The response of a single GTO during the activation of all MUs that produced the in-series effect has been compared with its discharge during activation of all the muscle's MUs (in-series and in-parallel) to demonstrate the existence of an in-parallel unloading effect (Binder 1981). Interestingly, the opposite observations were also reported; the whole muscle activation sometimes resulted in a larger GTO response than that when all in-series MUs were active. There seems to be general agreement that the in-series excitatory action predominates over any in-parallel effects (Proske 1993). In the ensemble of GTOs in a muscle, recruitment of additional MUs is always likely to produce an increase in total GTO activity because a MU that unloads one receptor will most probably activate another one (Horcholle-Bossavit et al. 1989). We chose not to model the in-parallel fiber unloading effect because it appears to be relatively small and inconsistent and its mechanism is unclear.

Comparison with previous modeling attempts

Several models of the GTO were proposed in the past and they used either transfer functions (Anderson 1974; Houk and Simon 1967; Lin and Crago 2002) or structural terms (Gregory and Proske 1981). The GTO models involving linear transfer functions are problematic because they attempt to relate the individual GTO afferent activity to the whole muscle force despite the fact that only a few of its MUs influence a given receptor's activity. These authors were primarily interested in modeling the nonlinear summation property during activation of progressively larger number of MUs, although such models fail to predict temporal patterns such as step changes observed when new MUs are gradually recruited. Finally, Lin and Crago modeled ensemble rather than individual GTO afferent activity, which is probably the information being used in calculations within the CNS (Crago et al. 1982; Houk and Henneman 1967; Reinking et al. 1975). Going directly to an ensemble model makes it difficult to use the model to predict changes in ensemble activity that might be associated with changes in fiber-type composition and innervation patterns such as occur during ontogenetic development and recovery from injury (Mileusnic and Loeb, unpublished observations).

Our model is somewhat simpler compared with others that have attempted to derive functional models from anatomical structure. Gregory and Proske (1981) suggested one such mechanical model in which a separate impulse-generating site was assumed for every muscle fiber inserting into the GTO. During the MU stimulation, a muscle fiber that inserts on collagen strands within the receptor capsule and on which the nerve terminals lie stretches a collagen strand and initiates activity in a terminal branch of the nerve. Stimulation of two muscle fibers together is assumed to initiate activity in two terminal branches, but the one with the higher rate of discharge suppresses (by antidromic invasion) the neighboring terminal by resetting. Although this produces complete occlusion, the researchers suggest that less-than-linear summation during combined stimulation is produced by cross-connections between collagen strands; both muscle fibers are effectively pulling on both nerve terminals and the strength of the cross-connections determines the size of the combined response. This model is somewhat speculative because it requires some 20 or 26 anatomically separate impulse-generating sites within a single cat's MG or soleus GTO, respectively, to account for its afferent behavior.

In conclusion, the GTO model accurately captures all salient aspects of GTO afferent behavior reported in the literature: static and dynamic responses to activation of single MUs whose muscle fibers insert into the GTO, self- and cross-adaptation, nonlinear summation when multiple MUs are active in muscle, and the proportional relationship between the cross-adaptation and summation recorded for various pairs of MUs.

Our GTO model is useful in several ways. Most directly, it can be used to generate a realistic representation of GTO afferent activity in larger models of neural control systems to provide better understanding of the actual control problems that must be solved by those systems. More generally, the GTO is a highly evolved example of a general class of mechanoreceptors in which collagen-based connective tissue structures direct and focus mechanical energy onto neural membrane transduction sites. At least some of the mechanical components and design principles of the GTO are likely to be found in other receptors for which mathematical models have yet to be defined.

We used the individual GTO model to study the ensemble properties of populations of GTOs. The information available to the CNS is derived from the aggregate activity of tens of GTO receptors in a typical muscle such as the feline MG. Although the individual GTO is strongly influenced by the vagaries of muscle fiber sampling and recruitment, the GTO aggregate activity may be a more reliable indicator of total muscle force. The aggregate activity will depend on factors such as the distributions of GTOs and muscle fiber types within the muscle (often highly heterogeneous) and the orderliness of MU recruitment (usually quite stable). To quantify these effects, we have combined our GTO model with models of normal and pathological neuromuscular architecture to obtain realistic representations of activity in populations of GTO receptors (Mileusnic and Loeb, unpublished observations).

APPENDIX

Apportioning muscle fiber insertion into innervated and bypassing regions of the GTO capsule

The fibers inserting into the GTO vary in size, especially in heterogeneous muscles like cat's MG. The average cross-sectional

areas of three types of fibers in cat's MG were measured to be 1,895 (S), 2,504 (FR), and 4,555 μm^2 (FF), whereas their tetanic tensions, estimated using a specific tension (32 N/cm^2; Scott et al. 1996), were estimated to be 0.606 (S), 0.801 (FR), and 1.454 mN (FF). We assumed that the amount of collagen that attaches to the fiber inserting into the GTO is proportional to its cross-sectional area, but only some of that collagen contributes to the innervated region and there is no reason for the percentage to be the same for all fibers. In fact, for the GTO to sample from such a large number of muscle fibers, there would seem to be a need for some organizational process to gather the collagen from those fibers into an orderly structure whose diameter is substantially smaller than the aggregate diameter of the muscle fibers themselves.

A geometrical arrangement representing the fibers inserting into the GTO was designed with the goal to apportion each fiber's collagen between the innervated and bypassing collagen (see Fig. 2*B*). The GTO's cross-sectional area was assumed to be flower-shaped with fibers being arranged in the manner of flower petals. In 1972 a detailed analysis was performed (Schoultz and Sweet 1972) in which the GTO's cross-sectional areas at different levels between the muscle and tendon end were studied. A single slice of muscle fibers that insert into the GTO capsule was also taken, but at some distance proximal to entering the capsule, at which point no clear evidence supporting any orderly arrangement of the fibers can be discerned. In the absence of direct anatomical evidence, we chose to design a conceptual flower-shaped model because of the indirect evidence arguing in favor of organized arrangement. In particular, even muscle fibers that insert halfway along the GTO capsule appear to be at no disadvantage in generating responses in the GTO afferent (Spielmann and Stauffer 1986). This suggests that there is some trophic mechanism to direct a specific proportion of the collagen arising from the termination of each muscle fiber into the transduction zone in the center of the GTO.

To design the flower-shaped area, we assumed that for all the fibers inserting into the receptor, the ratio of each petal-shaped area's radius and subtended angle (R and θ) remains the same (see Fig. 2*B*)

$$\frac{r_1}{r_2} = \frac{\theta_1}{\theta_2}$$

In other words, the fiber having the larger total cross-sectional area was assumed to have both a larger angle and radius of the petal-shaped area than those of the smaller fiber. Simple geometry then dictates that the fiber having f times larger (smaller) cross-sectional area than that of the other fiber will have $\sqrt[3]{f}$ times larger (smaller) r and θ than the other fiber. In other words if $A_2 = f \times A_1$ (where A_1 and A_2 are the cross-sectional areas of two different fibers), then $(\theta_2 \times r_2 \times r_2)/2 = f \times (\theta_1 \times r_1 \times r_1)/2$. By substituting $r_2 = (r_1 \times \theta_2)/\theta_1$ into the previous equation we get the following relationships: $\theta_2/\theta_1 = \sqrt[3]{f}$ and $r_2/r_1 = \sqrt[3]{f}$.

The individual fiber's angle of its petal-shaped area was calculated in several steps. First, the smallest fiber in the GTO was assigned to have the petal angle equal to x, whereas for all the larger fibers in the GTO the cube root of the ratio of its area and the smallest fiber's area were calculated to obtain its petal angle ($\sqrt[3]{A^f/A^f_{smallest}} \times x$, where A^f is the fiber's total cross-sectional area and $A^f_{smallest}$ is the smallest fiber's cross-sectional area). The values of the petal angles of all fibers in the GTO were summed together and set to equal 2π to obtain the smallest fiber's petal angle x ($x = 2\pi/\sum_{f=1}^{11} \sqrt[3]{A^f/A^f_{smallest}}$). The remaining fibers' petal angles were obtained by multiplying x by the cube root of the ratio of the individual fiber's cross-sectional area to the smallest fiber's cross-sectional area.

The amount of innervated collagen derived from each muscle fiber (A^{f_inner}) was obtained by multiplying its fiber's petal angle ($\theta^f = x \times \sqrt[3]{A^f/A^f_{smallest}}$) by the radius of area of the GTO's total innervated collagen (radius of the area that is equal to 10% of the total GTO area; see *Construction of the model* and *Parameter determination*).

The amount of each muscle fiber's collagen that contributes to the bypassing type was determined by subtracting the fiber's innervated collagen from its total collagen ($A^{f\_bypass} = A^f - A^{f\_inner}$).

REFERENCES

Alneas E. Static and dynamic properties of Golgi tendon organs in the anterior tibial and soleus muscles of the cat. *Acta Physiol Scand* 70: 176–187, 1967.

Anderson JH. Dynamic characteristics of Golgi tendon organs. *Brain Res* 67: 531–537, 1974.

Banks R, Hulliger M, Scheepstra KA, and Otten E. Pacemaker activity in a sensory ending with multiple encoding sites: the cat muscle spindle primary ending. *J Physiol* 498: 177–199, 1997.

Barker D. The morphology of muscle receptors. In: *Handbook of Sensory Physiology*, edited by Hunt CC. Berlin: Springer-Verlag, 1974, vol. 3, pt. 2, p. 1–190.

Binder MD. Further evidence that the Golgi tendon organ monitors the activity of a discrete set of motor units within a muscle. *Exp Brain Res* 43: 186–192, 1981.

Brown IE, Scott SH, and Loeb GE. Mechanics of feline soleus: II. Design and validation of mathematical model. *J Muscle Res Cell Motil* 17: 221–233, 1996.

Burke RE. Motor units: anatomy, physiology and functional organization. In: *Handbook of Physiology: The Nervous System. Motor Control*. Bethesda, MD: Am. Physiol. Soc., 1981, sect. 1, vol. II, pt. 1, p. 345–422.

Burke RE and Tsairis P. Anatomy and innervation ratios in motor units of cat gastrocnemius. *J Physiol* 234: 749–765, 1973.

Carr RW, Gregory JE, and Proske U. Summation of responses of cat muscle spindles to combined static and dynamic fusimotor stimulation. *Brain Res* 800: 97–104, 1998.

Crago PE, Houk JC, and Rymer WZ. Sampling of total muscle force by tendon organs. *J Neurophysiol* 47: 1069–1083, 1982.

Fallon JB, Carr RW, Gregory JE, and Proske U. Summing responses of cat soleus muscle spindles to combined static and dynamic fusimotor stimulation. *Brain Res* 888: 348–355, 2001.

Fukami Y and Wilkinson RS. Responses of isolated Golgi tendon organs of the cat. *J Physiol* 265: 673–689, 1977.

Gandevia SC. Kinesthesia: roles for afferent signals and motor commands. In: *Handbook of Physiology. Exercise: Regulation and Integration of Multiple Systems. Neural Control of Movement.* Bethesda, MD: Am. Physiol. Soc., 1996, sect. 12, pt. 1, chapt. 4, p. 128–172.

Goldfinger MD and Fukami Y. Interaction of activity in frog skin touch afferent units. *J Neurophysiol* 45: 1096–1108, 1981.

Golgi C. Intorno alla distribuzione e terminazione dei nervi nei tendini dell'uomo e di altri vertebrati. *Rend R Ist Lomb Sci Lett* B11: 445–453, 1878.

Golgi C. Sui nervi dei tendini dell'uomo et di altri vertebrati e di un nuovo organo nervosa terminale muscolo-tendineo. *Mem R Acad Sci Torino* 32: 359–385, 1880.

Gregory JE. Relations between identified tendon organs and motor units in the medial gastrocnemius muscle of the cat. *Exp Brain Res* 81: 602–608, 1990.

Gregory JE, Morgan DL, and Proske U. Site of impulse initiation in tendon organs of cat soleus muscle. *J Neurophysiol* 54: 1383–1395, 1985.

Gregory JE, Morgan DL, and Proske U. The discharge of cat tendon organs during unloading contractions. *Exp Brain Res* 61: 222–226, 1986.

Gregory JE and Proske U. The responses of Golgi tendon organs to stimulation of different combination of motor units. *J Physiol* 295: 251–262, 1979.

Gregory JE and Proske U. Motor unit contractions initiating impulses in a tendon organ in the cat. *J Physiol* 313: 251–262, 1981.

Horcholle-Bossavit G, Jami L, Petit J, Vejsada R, and Zytnicki D. Ensemble discharge from Golgi tendon organs of cat peroneus tertius muscle. *J Neurophysiol* 64: 813–821, 1990.

Houk JC and Henneman E. Responses of Golgi tendon organs to active contraction of the soleus muscle of the cat. *J Neurophysiol* 30: 466–481, 1967.

Houk JC and Simon W. Responses of Golgi tendon organs to forces applied to muscle tendon. *J Neurophysiol* 30: 1466–1481, 1967.

Ito F, Kanamori N, and Kuroda H. Structural and functional asymmetries of myelinated branches in the frog muscle spindle. *J Physiol* 241: 389–405, 1974.

Jami L. Golgi tendon organs in mammalian skeletal muscle: functional properties and central action. *Physiol Rev* 72: 623–661, 1992.

Lin CK and Crago PE. Neural and mechanical contributions to the stretch reflex: a model synthesis. *Ann Biomed Eng* 30: 54–67, 2002.

Lund JP, Richmond FJR, Touloumis C, Patry Y, and Lamarre Y. The distribution of Golgi tendon organs and muscle spindles in messeter and temporalis muscles of the cat. *Neuroscience* 3: 259–270, 1978.

Mileusnic M, Brown IE, Lan N, and Loeb GE. Mathematical models of proprioceptors. I. Control and transduction in the muscle spindle. *J Neurophysiol* 96: 1772–1788, 2006.

Nitatori T. The fine structure of human Golgi tendon organs as studied by three-dimensional reconstruction. *J Neurocytol* 17: 27–41, 1988.

Proske U. The Golgi tendon organ. In: *Peripheral Neuropathy*, edited by Dyck P, Thomas P, Griffin I, Low P, and Podusko I. Philadelphia, PA: Saunders, 1993, p. 141–148.

Proske U and Gregory JE. The discharge rate: tension relation of Golgi tendon organs. *Neurosci Lett* 16: 287–290, 1980.

Reinking RM, Stephens JA, and Stuart DG. The tendon organs of cat medial gastrocnemius: significance of motor unit type and size for activation of Ib afferent. *J Physiol* 250: 491–512, 1975.

Richmond FJR. *Dorsal Muscles of the Cat Neck: Their Morphology, Their Histochemistry and the Nature of Their Encapsulated Sensory Receptors* (MS thesis). Kingston, Ontario, Canada: Queen's Univ. Press, 1974.

Richmond FJR and Stuart DG. Distribution of sensory receptors in the flexor carpi radialis muscle of the cat. *J Morphol* 183: 1–13, 1985.

Schoultz TW and Swett JE. The fine structure of the Golgi tendon organ. *J Neurocytol* 1: 1–26, 1972.

Schoultz TW and Swett JE. Ultrastructural organization of the sensory fibers innervating the Golgi tendon organ. *Anat Rec* 179: 147–162, 1973.

Scott SH, Brown IE, and Loeb GE. Mechanics of feline soleus: I. Effect of fascicle length and velocity on force output. *J Muscle Res Cell Motil* 17: 207–219, 1996.

Scott SH and Loeb GE. Mechanical properties of the aponeurosis and tendon of the cat soleus muscle during whole-muscle isometric contractions. *J Morphol* 224: 73–86, 1995.

Spielmann JM and Stauffer EK. Morphological observations of motor units connected in series to Golgi tendon organs. *J Neurophysiol* 55: 147–162, 1986.

Stuart DG, Mosher CC, Gerlach RL, and Reinking RM. Mechanical arrangement and transducing properties of Golgi tendon organs. *Exp Brain Res* 14: 274–292, 1972.

Swett JE and Eldred E. Distribution and numbers of stretch receptors in medial gastrocnemius and soleus muscles of the cat. *Anat Rec* 137: 453–460, 1960.